

~~B~~ n

## DISTRIBUTION STATEMENT A

Approved for public release  
Distribution Unlimited

*by A. C. Kyser*

19960327 113

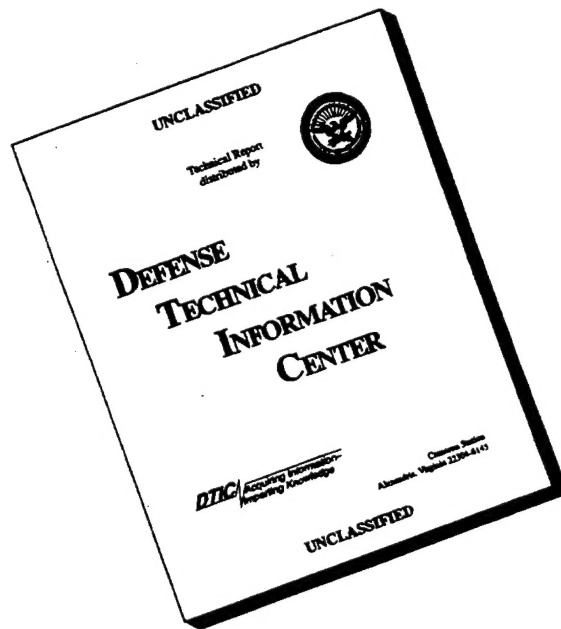
DTIC QUALITY INSPECTED 1

DEPARTMENT OF THE ARMY  
PLASTICS TECHNICAL EVALUATION CENTER  
PICATINNY ARSENAL, DOVER, N. J.

OCT.  
64

OCT 6

# DISCLAIMER NOTICE



**THIS DOCUMENT IS BEST QUALITY AVAILABLE. THE COPY FURNISHED TO DTIC CONTAINED A SIGNIFICANT NUMBER OF PAGES WHICH DO NOT REPRODUCE LEGIBLY.**

THE UNIFORM-STRESS SPINNING FILAMENTARY DISK

By A. C. Kyser

Distribution of this report is provided in the interest of information exchange and should not be construed as endorsement by NASA of the material presented. Responsibility for the contents resides in the author or organization that prepared it.

Prepared under Contract No. NASw-652 by  
ASTRO RESEARCH CORPORATION  
Santa Barbara, Calif.

for

NATIONAL AERONAUTICS AND SPACE ADMINISTRATION

~~For sale by the Office of Technical Services, Department of Commerce,  
Washington, D.C. 20230 -- Price \$0.75~~

DTIC QUALITY INSPECTED 1

## CONTENTS

	<u>Page</u>
ABSTRACT	1
SECTION I NOMENCLATURE	2
SECTION II INTRODUCTION	3
SECTION III DEVELOPMENT OF THE CURVATURE EQUATION	5
SECTION IV INTEGRATION OF CURVATURE EQUATION	8
SECTION V DETERMINATION OF ARC LENGTH	10
SECTION VI DETERMINATION OF CENTRAL ANGLE	11
SECTION VII DISCUSSION OF CURVE SHAPE	12
REFERENCES	16

## ABSTRACT

[An analysis is presented for the development of the fiber patterns necessary to produce uniform fiber tension in a spinning filamentary disk. The family of fiber patterns for such isotenoid disks is described in terms of curvature, slope, and arc length, and means are suggested for obtaining polar-coordinate plots of the patterns. Included are diagrams of three of the patterns, a photograph of a model, and a discussion of the general characteristics of the family of allowable patterns. It was found that the isotenoid disk design with which the disk is covered by uniform-diameter fibers operates at half the stress of a simple hoop, for a given tip speed and fiber mass per unit length.

*There are 5 subfigures and 4 figures. (4 in 1)*

# I. NOMENCLATURE

$r$	—	radius coordinate
$r_o$	—	radius of disk
$R$	—	$r/r_o$ , nondimensional radius coordinate
$\beta$	—	angle between fiber and radius vector
$\rho$	—	radius of curvature of fiber
$\omega$	—	rotation speed of disk
$m'$	—	mass per unit length along fiber
$\Omega$	—	$m'\omega^2 r_o^2 / T$ , fiber loading parameter
$F'$	—	interfiber shear force per unit length
$T$	—	tension in structural fiber
$\theta$	—	angle swept by tangent to fiber
$\varphi$	—	central angle coordinate
$\ell$	—	arc length along fiber, measured from periphery of disk
$L$	—	$\ell/r_o$ nondimensional arc length
$\chi$	—	$R^2$ , nondimensional radius coordinate
$s$	—	stress in structural fiber
$\gamma$	—	weight density of fiber material
$\lambda$	—	$s/\gamma$ , specific strength of fiber
$v_o$	—	tip speed of rotating disk

## II. INTRODUCTION

This note presents the analytical development of a uniform-stress (isotenoid) spinning disk composed of structural filaments of uniform cross section. The filamentary arrangement is that of a fine-mesh circular net in which the fibers form curved load-carrying paths that spiral outward from the center. It can be shown that any spiral net will carry a radially-directed loading in such a way that the resultant fiber tension decreases toward the center of the net. This tension gradient is the result of the spiral load-path curvature. The fiber tension resulting from the inertia forces due to rotation, on the other hand, tends to increase toward the center. The constant-tension condition can be imposed by arranging for the curvature distribution to be that which is necessary to allow these two tension-gradient effects to cancel.

This work may be considered an extension of the work done in References 1 and 2. In Reference 1 a theory was developed for predicting equilibrium shapes of filamentary structures in which the structural loads are carried in pure tension. This paper was specifically concerned with normal loads on the fiber (i. e., pressure loads), and the solutions were presented in terms of differential equations describing the local curvature and/or slope of the structural wall in terms of

the local conditions. In Reference 2 this problem was generalized to include load components tangential to the structural wall (from centrifugal effects), and solutions for the curvature and slope equations were obtained in the form of elliptic integrals. The present note represents a further generalization, in that allowance is made for an internally-generated shear stress in the filamentary wall.

This type of structure is proposed for space applications where requirements exist for large rotating surfaces in which the loads generated by the mass of rotating structure are important. One such application is suggested by Reference 3, which discusses the use of a lightweight woven fabric net as a low-loading, low-temperature, rotating wing for re-entry deceleration. Other possible applications include the use of filamentary disks to support large surfaces for the collection or reflection of radiant energy. It is believed that an isotenoid disk of this type, in addition to having the excellent mechanical properties characteristic of filamentary structures, can be made to have a high structural efficiency.

The work reported here was conducted with the financial support of the National Aeronautics and Space Administration.



### III. DEVELOPMENT OF THE CURVATURE EQUATION

The structure under consideration is a spinning filamentary disk having the form of symmetrical spiral net with a differentially-fine mesh, the clockwise-outward-directed fibers being attached point-by-point to the counterclockwise-outward fibers. A typical intersection between opposing fibers is shown in Figure 1. Each branch has a local radius of curvature  $\rho$  and meets the radius vector at an angle  $\beta$ .

The forces acting on a differential length  $d\ell$  of the clockwise-outward fiber are shown in Figure 2. The tension forces, shown dashed, are added and resolved into forces normal to and tangential to the fiber,  $T d\ell/\rho$  and  $dT$ . The radially-directed inertia force is  $m'\omega^2 r d\ell$ , where  $m'$  is the mass per unit length. The force  $F'd\ell$  is the interfiber shear force, or the force exerted on the element of the clockwise-outward fiber by the corresponding counterclockwise fiber. This force must be equal and opposite to the force on the counterclockwise element at this point. For reasons of symmetry, then, it must lie in the circumferential direction, normal to the radius vector.

From the diagram it can be seen that equilibrium requires that

$$m'\omega^2 r d\ell \sin\beta + F'd\ell \cos\beta = \frac{T}{\rho} d\ell \quad (1)$$

and

$$m' \omega^2 r \, d\ell \cos \beta - F' d\ell \sin \beta = \frac{dT}{d\ell} d\ell \quad . \quad (2)$$

Equations (1) and (2) can be simplified by calling

$$\Omega \equiv \frac{m' \omega^2 r_o^2}{T} \quad (3)$$

$$R \equiv \frac{r}{r_o} \quad .$$

The uniform-stress condition can be imposed by making  $\Omega = \text{const.}$  , assuming that the structural cross section of the fiber is proportional to the mass per unit length. If it is assumed, further, that  $m' = \text{const.}$  , then  $T = \text{const.}$  , and

$$\frac{dT}{d\ell} = 0 \quad . \quad (4)$$

Equations (1) and (2) then reduce to

$$\frac{\rho}{r_o} = \frac{\sin \beta}{\Omega R} \quad (5)$$

and

$$F' = \frac{m' \omega^2 r}{\tan \beta} = \frac{\Omega R}{\tan \beta} \frac{T}{r_o} \quad . \quad (6)$$

Equation (5) is sufficient to define the geometry of the fiber pattern for any given value of the parameter  $\Omega$  . It is possible to establish the family of patterns, without further analytical work, from this radius of curvature equation by a graphical integration process using a compass and protractor.

The structural requirement for transferring shear between fibers can be seen from Equation (6). It should be noted that the path of a given fiber need not actually follow a continuous spiral, but may instead follow a zigzag pattern, in the circumferential direction, between adjacent circles of intersections. For this type of fiber pattern, there is no tendency for the intersection to slide, and therefore there is no requirement for transferring shear.

#### IV. INTEGRATION OF CURVATURE EQUATION

Equation (5) can be integrated to give a relation for  $\rho$  (or  $\sin\beta$ ) as a function of  $r$  as follows: From Figure 3 it can be seen that

$$d\beta = (\beta + d\beta) - \beta = d\theta - d\varphi .$$

Also, 
$$d\theta = \frac{dr}{\rho \cos\beta} ; \quad d\varphi = \frac{dr \tan\beta}{r} .$$

Consequently, 
$$\frac{d\beta}{dr} = \frac{1}{\rho \cos\beta} - \frac{\tan\beta}{r} ,$$

or, 
$$\frac{d\beta}{dR} \cos\beta = \frac{r_0}{\rho} - \frac{\sin\beta}{R} . \quad (7)$$

Equation (7) can, of course, be obtained from the standard form of the radius of curvature in polar coordinates. This relation can be combined directly with Equation (5) to eliminate  $d\beta/dr$  if (5) is expressed in a differentiated form:

$$\cos\beta \frac{d\beta}{dR} = \frac{\Omega}{r_0} R \frac{d\rho}{dR} + \frac{\Omega}{r_0} \rho . \quad (5a)$$

Equating (5a) to (7) and substituting Equation (5) to eliminate  $\beta$  gives a separable linear differential equation in  $\rho(R)$  :

$$\frac{2\rho d\rho}{\rho^2 - \frac{r_0}{2\Omega}} = -4 \frac{dR}{R} . \quad (8)$$

In integrating this expression, the initial conditions are taken as those at the point at which the fiber is tangent to the outer periphery:

$R = R_o = 1$  ,  $\beta = \beta_o = \pi/2$  . Here  $\rho_o = r_o/\Omega$  . These conditions establish the upper limits for the integration. The lower limits are taken at the generic point along the fiber curve. This process gives for the radius of curvature

$$\frac{\rho^2}{r_o^2} = \frac{1}{2\Omega} \left[ 1 + \left( \frac{2 - \Omega}{\Omega} \right) \frac{1}{R^4} \right] . \quad (9)$$

If this expression is combined with Equation (5), it gives

$$\sin^2 \beta = \frac{\Omega R^2}{2} \left[ 1 + \left( \frac{2 - \Omega}{\Omega} \right) \frac{1}{R^4} \right] . \quad (10)$$

Either of Equations (9) or (10) suffices to describe the fiber pattern for graphical integration; Equation (9) may be used in a step-wise forward integration with a compass, while Equation (10) may be used to construct a slope field through which a continuous path may be faired.

## V. DETERMINATION OF ARC LENGTH

The arc length  $\ell$  included between two points along the curve can be established by an integration of the relation

$$d\ell = \frac{dr}{\cos \beta} = \frac{dr}{\sqrt{1 - \sin^2 \beta}}, \quad (11)$$

which can be written by inspection of Figure 3. If Equation (10) is substituted for  $\sin \beta$ , and if the independent variable is changed to  $\chi = R^2$ , then the nondimensional arc length  $L$  can be expressed as the integral

$$L = \frac{1}{\sqrt{2\Omega}} \int_{R^2}^1 \frac{d\chi}{\sqrt{-\chi^2 + \frac{2}{\Omega}\chi - \left(\frac{2-\Omega}{\Omega}\right)}}. \quad (12)$$

This integral is evaluated in Reference 4. After accounting for the limits, it is possible to express the arc length as

$$L = \frac{1}{\sqrt{2\Omega}} \left[ \frac{\pi}{2} + \sin^{-1} \left( \frac{1 - \Omega R^2}{\Omega - 1} \right) \right]. \quad (13)$$

Equation (13) is extremely useful in making graphical constructions of fiber patterns, in that it provides a reference to the starting point which is not affected by cumulative errors in the graphical integration process.

## VI. DETERMINATION OF CENTRAL ANGLE

The determination of the central angle  $\varphi$  is desirable to complete the description of the fiber patterns. To find  $\varphi$  as a function of  $R$  it is necessary to integrate the expression (see Figure 3)

$$d\varphi = \frac{\sin\beta}{R} \frac{d\ell}{dR} dR \quad . \quad (14)$$

If the appropriate expressions are substituted into Equation (14) to define  $d\varphi$  as a function of  $R$  and then the substitution  $\chi = R^2$  is made, the result is the integral

$$2\varphi(R) = \int_{R^2}^1 \frac{\chi d\chi}{\sqrt{(-\chi^2 + \beta\chi - C)(\chi^2 + C)}} + \int_{R^2}^1 \frac{C d\chi}{\chi \sqrt{(-\chi^2 + \beta\chi - C)(\chi^2 + C)}} \quad (15)$$

where  $\beta \equiv \frac{2}{\Omega} \quad ; \quad C \equiv \frac{2}{\Omega} - 1 \quad .$

These integrals are evaluated in Reference 5 in terms of the elliptic integral of the third kind. The solution for the  $\Omega > 2$  cases differs from that for the  $\Omega < 2$  cases because of the difference in the nature of the roots of the quartic under the radical. There are, therefore, four different integrals to be evaluated, each of which has its own set of coefficients in terms of the roots of the quartic. Consequently, this description of the curve family is somewhat unmanageable. Further details of this solution will therefore be omitted.

## VII. DISCUSSION OF CURVE SHAPE

Equations (9) and (10) can be used to identify two distinct types of curves in the one-parameter family which includes  $\Omega \geq 1$ . (Note that  $\Omega < 1$  produces a contradiction, since it gives  $\rho_0 > r_0$ , which requires that  $r = r_0$  be a local minimum instead of maximum.) These two curve types are bounded by  $\Omega = 2$ : for  $\Omega < 2$ ,  $\rho$  must increase with decreasing  $R$ , and for  $\Omega > 2$ ,  $\rho$  must decrease. The former ( $\Omega < 2$ ) condition produces an annular band of fiber paths, as in Figure 4 ( $\Omega = 3/2$ ), which are characterized by smooth, continuously-turning curves that are tangent alternately to the outer periphery and some inner periphery. The radius of the inner periphery can be found by setting  $\sin\beta = 1$  in Equation (10). This gives

$$R_{\min}^2 = \frac{2}{\Omega} - 1. \quad (16)$$

For  $\Omega = 1$ , Equation (9) gives  $\rho_0 = r_0$ , which is simply the circular hoop.

The  $\Omega = 2$  case has special importance because it is the only case which includes the origin and therefore covers the disk. For this case,  $\rho = r_0/2 = \text{const.}$ , and the fiber curve is simply a circle tangent to the periphery and passing through the origin. This pattern, which is diagrammed in Figure 5, was the one chosen for the model



shown photographed in Figure 6. This pattern has the somewhat startling property that it can be mapped, without changes in arc lengths, from a rectangular net having a length-to-width ratio of four, and consisting of square meshes at  $45^\circ$  to the axis of the rectangle, as shown in Figure 7. This property arises from the fact that two circular fiber paths, whose centers are displaced on the disk by a central angle  $\varphi$ , intersect at values of arc length  $\ell = 2\rho\varphi = r_o\varphi$ ; for a center displacement of  $2\varphi$ , the arc lengths to the intersections are  $\ell = 2r_o\varphi$ ; etc.

The curves  $\Omega > 2$  are characterized by the fact that  $\sin\beta$  and  $\rho$  both vanish at some value of  $R$ ; these curves have radially-directed cusps at a value of  $R$  which can be determined by setting either  $\rho$  or  $\sin\beta$  to zero in Equations (9) or (10). This gives

$$R_{\min}^4 = 1 - \frac{2}{\Omega} . \quad (17)$$

Figure 8 shows the fiber pattern for  $\Omega = 3$ .

The  $\Omega > 2$  curves are not structurally self-sufficient; each cusp must be supported by a radial force of  $2T$ . These radial forces could be provided by radial spokes, a hoop, or a fiber system comprised of any one of the  $\Omega > 1$  curves properly truncated to allow for residual radial forces at the truncation radius.

The truncation process can, of course, be applied to both the inner and outer peripheries of an annular band of a spiral net. Such

a band could be spliced at its two peripheries to other similar bands (having the same fiber stress, for example). In general, these neighboring bands would each have a different reference radius  $r_o$  and a different  $\Omega$ . This process, taken to the limit, could be used to produce a uniform-stress disk using tapered filaments.

The parameter  $\Omega$  establishes the relation between tip speed  $v_o = \omega_o r_o$  and fiber stress  $s$ . The maximum tip speed  $(v_o)_{ult}$  of which a disk of a given material is capable can be determined by substituting the specific strength  $\lambda$  of the structural material for the ratio of breaking strength  $T_{ult}$  to mass per unit length, as follows:

$$\lambda \equiv \frac{s_{ult}}{\gamma} \cdot \frac{A_f}{A_f} = \frac{T_{ult}}{m'g} \quad (18)$$

where  $\gamma$  is the weight density of the material and  $A_f$  is the cross-sectional area of the fiber. If this condition is substituted into Equation (3), which defines  $\Omega$ , the ultimate tip speed is seen to be

$$(v_o)_{ult} = \sqrt{g \lambda \Omega} \quad (19)$$

Thus a higher  $\Omega$  allows a higher ultimate tip speed.

If the radius of the hub is given, the choice of  $\Omega$  is narrowed to a range of values given by Equation (10) by setting  $\sin^2 \beta$  at the limits of 1 and 0. These values of  $\Omega$  are those determined by Equations (16) and (17). For intermediate values of  $\Omega$  the fiber curve will intersect the hub radius at an angle  $\beta$  which can be determined from Equation (10). Since the radial component of fiber tension,  $T \cos \beta$ , must be carried

by the hub, the load-carrying ability of the hub may be used to determine  $\Omega$  uniquely.

It should be recognized that the conditions governing the design of filamentary disks for use as items of hardware are likely to be such that the idealized disk analyzed here is only a point of departure. As an example, if the disk structure were required to support a reflective surface, then  $m'$  would probably be dependent on radius. For such a case the details of the solution given here will have to be modified. The basic curvature equation is general, however, and solutions can be extracted for any set of conditions that can be defined explicitly in terms of radius.

## REFERENCES

1. Schuerch, H., Burggraf, O. R., Kyser, A. C., A Theory and Applications of Filamentary Structures, NASA TN D-1692, December 1962.
2. Burggraf, O. R. and Schuerch, H., Analysis of Axisymmetric Rotating Pressurized Filamentary Structures, NASA TN D-1920, May 1963.
3. Schuerch, H. and MacNeal, R., Low Density, Autorotating Wings for a Manned Re-entry, Engineering Problems of Manned Interplanetary Exploration (a volume of technical papers presented September 30 - October 1, 1963, Palo Alto, Calif.), Amc. Inst. of Aeronautics and Astronautics, October 1963.
4. Pierce, B. O. and Foster, R. M., A Short Table of Integrals, Ginn and Company, 1957.
5. Byrd, P. F. and Friedman, M. D., Handbook of Elliptic Integrals for Engineers and Physicists, Springer-Verlag, 1954.

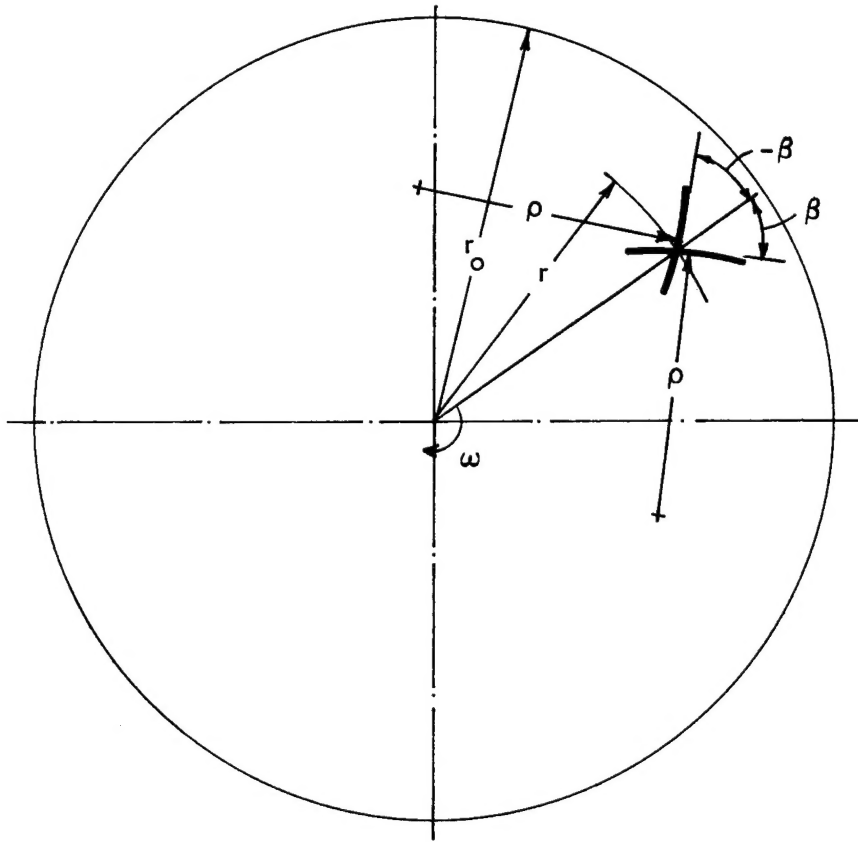


Figure 1. Local Geometry of Fiber Pattern.

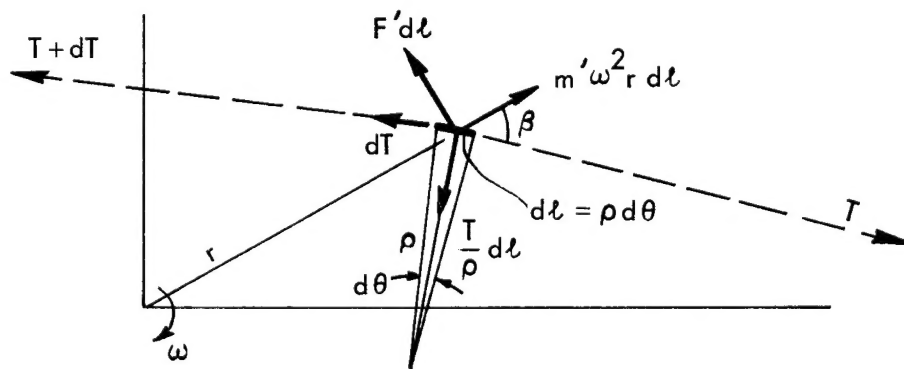


Figure 2. Forces on Fiber Element.

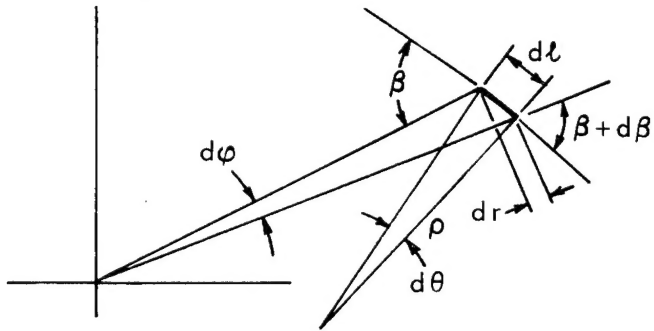


Figure 3. Radius of Curvature in Polar Coordinates.

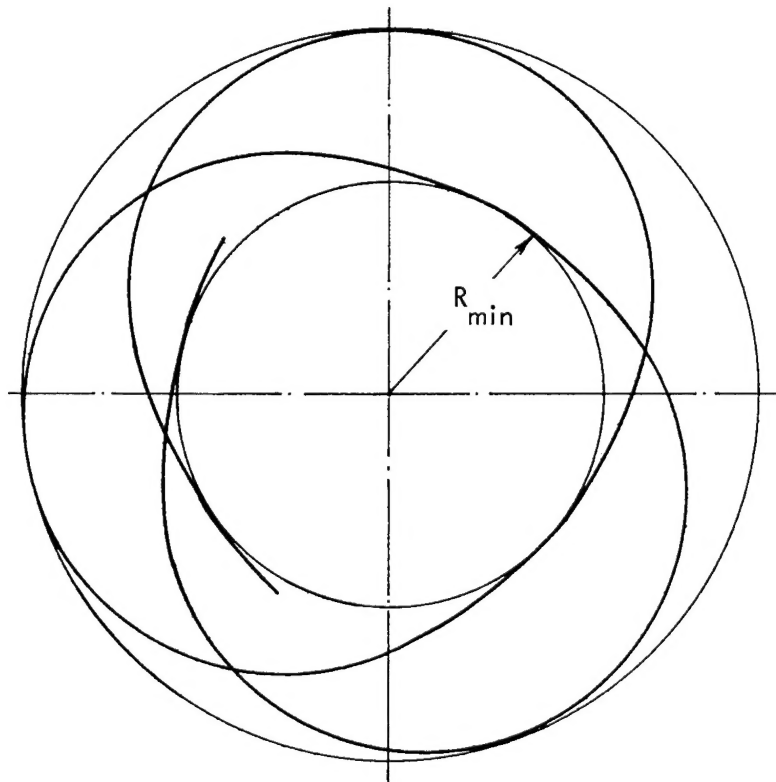


Figure 4. Fiber Pattern for Isotenoid Disk,  $\Omega = \frac{3}{2}$ .

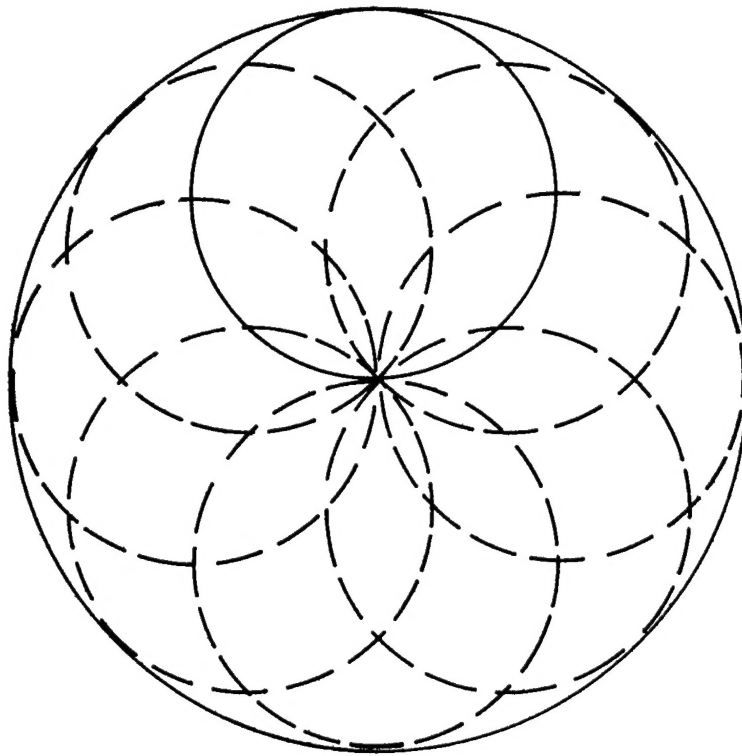


Figure 5. Fiber Pattern for Isotensoid Disk,  $\Omega=2$  .

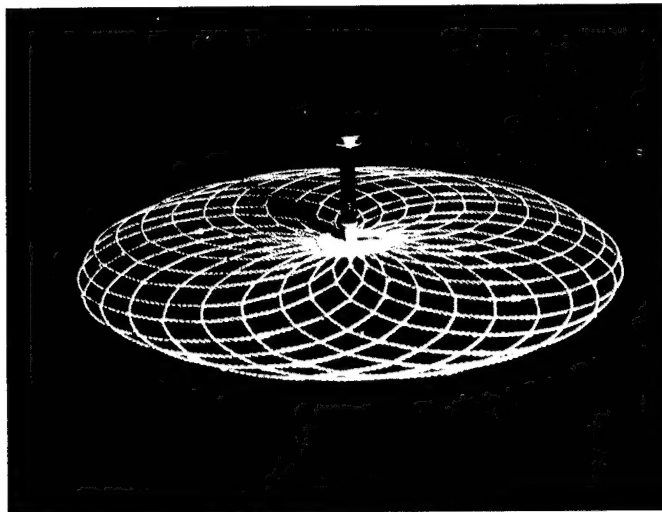


Figure 6. Photograph of Model Isotensoid Disk on Spin Stand.

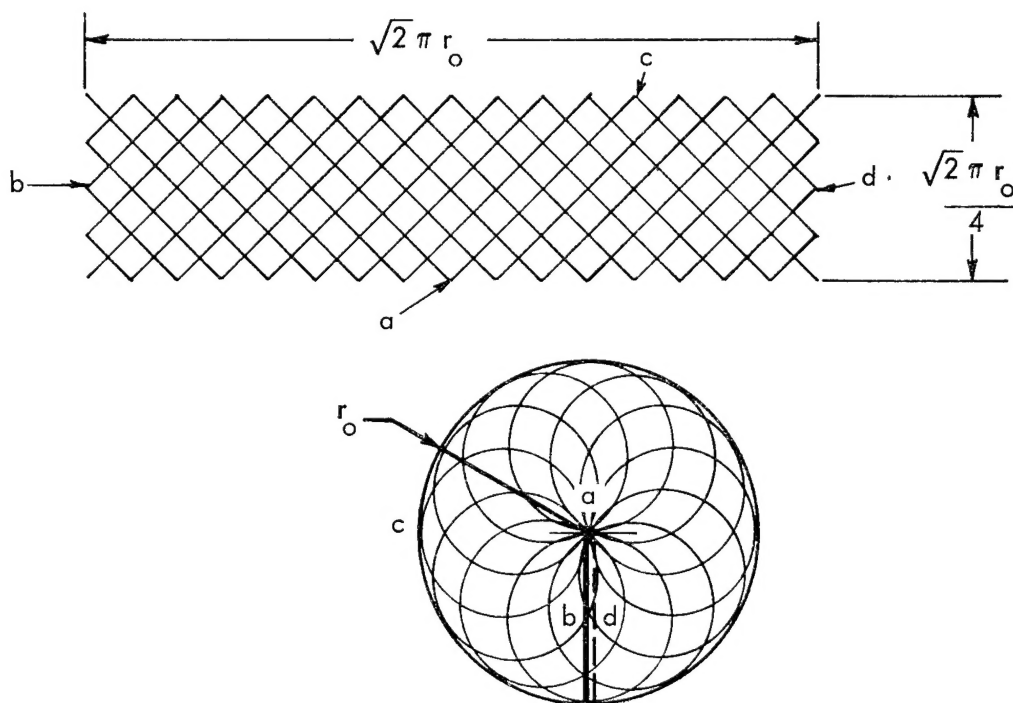


Figure 7. Mapping of Rectangular Net into  $\Omega=2$  Isotensoid Disk.

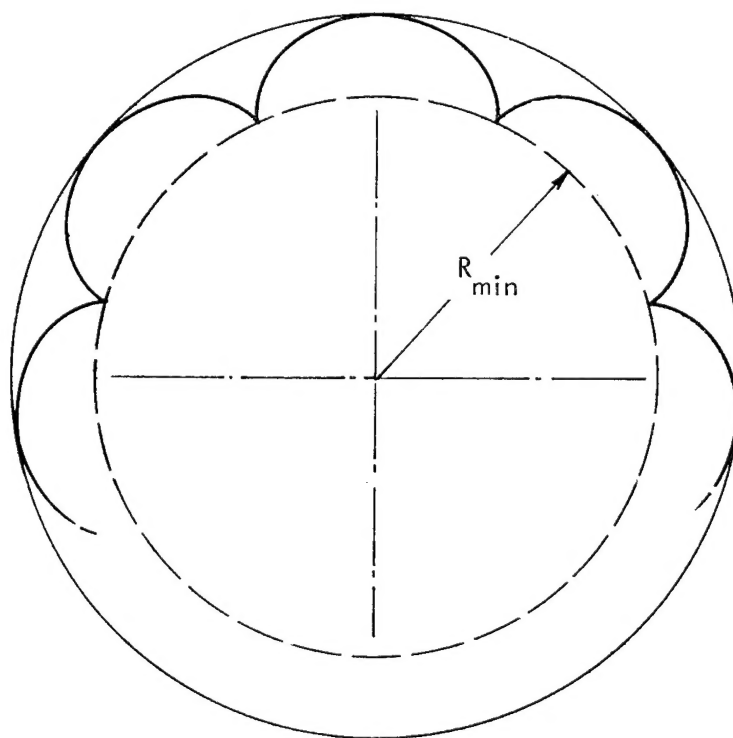


Figure 8. Fiber Pattern for Isotensoid Disk,  $\Omega=3$ .